Structure and Dissociation Energy of Weakly Bound H$_{2n+1}^+$ ($n = 5$–8) Complexes

HYUN-IL SEO,[1] JU-YONG SUN,[1] CHANG-HO SHIN,[2] SEUNG-JOON KIM[1]

[1]*Department of Chemistry, HanNam University, Daejeon 300-791, Korea*

[2]*KT&G Central Research Institute, Daejeon 305-805, Korea*

ABSTRACT: The geometrical parameters, vibrational frequencies, and dissociation energies for H$_{2n+1}^+$ ($n = 5$–8) clusters have been investigated using high level ab initio quantum mechanical techniques with large basis sets. The highest level of theory employed in this study is TZ2P CCSD(T). The C_1 structure of H$_{15}^+$ is predicted to be a global minimum, while the C_s structure of H$_{15}^+$ is calculated to be a transition state. Harmonic vibrational frequencies are also determined at the DZP and TZ2P CCSD levels of theory. The dissociation energies, D_e, for H$_{2n+1}^+$ ($n = 5$–8) have been predicted using energy differences at each optimized geometry, and zero-point vibrational energies (ZPVEs) are considered to compare with experimental values. The dissociation energies (D_o) have been predicted to be 1.69, 1.65, 1.65, and 1.46 kcal · mol for H$_{11}^+$, H$_{13}^+$, H$_{15}^+$ (C_1 symmetry) and H$_{17}^+$, respectively, at the TZ2P CCSD(T) level of theory. © 2006 Wiley Periodicals, Inc. Int J Quantum Chem 107: 988–997, 2007

Key words: ab initio; hydrogen clusters; dissociation energies; TZ2P CCSD(T)

Introduction

H$_{2n+1}^+$ clusters are weakly bound complexes composed by attaching the $n - 1$ number of H$_2$ molecule systemically around the three-membered ring of the H$_3^+$ ion. These kinds of complexes are very difficult to be found at normal condition experimentally because of their instability, but there is a possibility to exist at the special condition of ~3 K in absolute temperature and 0 bar in pressure.

$$H_3^+(H_2)_{n-1} + H_2 \rightleftharpoons H_3^+(H_2)_n \qquad (n = 1, 2, 3, \dots).$$
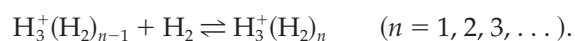
The parent H$_{2n+1}^+$ cluster, H$_3^+$ was first observed by Thompson [1], Krasoski [2] proposed the existence of hydrogen clusters in the interstellar medium. Drossart [3] and Miller et al. [4] observed the infrared (IR) spectrum of H$_3^+$ emitted from the atmo-

Correspondence to: S.-J. Kim; e-mail: sjkim@chem.hannam.ac.kr

sphere of Jupiter in 1989 and supernova SN 1987 in 1992, respectively.

Experimental investigations for H_{2n+1}^+ ($n \geqq 2$) series have become serious since 1960. In 1969, Clampitt and Gowland discovered H_5^+ to H_{47}^+ using mass spectrometry at 3 K in temperature and $\sim 10^{-10}$ mm Hg pressure. They reported that H_{15}^+ has been found to be the most abundant ion cluster, which suggests that it is particularly stable [5]. In 1973, Van Deurson and Reuss [6] proposed that odd-numbered clusters are ~ 50 times more stable than even-numbered clusters. Because of this, investigation for the odd-numbered hydrogen clusters was generally performed. The molecular structures and stabilities of H_5^+–H_{11}^+ were determined using a pulsed electron-beam mass spectrometer by Hiraoka and Kebarle [7] in 1975. In 1987, they expanded their study up to H_{21}^+ and concluded that the ions H_5^+, H_9^+, H_{15}^+, and H_{19}^+ are relatively more stable toward dissociation [8]. They reported that the binding energies were determined to be 1.72 kcal · mol for H_{11}^+, 1.64 kcal · mol for H_{13}^+, 1.54 kcal · mol for H_{15}^+, and 0.88 kcal · mol for H_{17}^+. The next year, the H_2 stretching vibrational frequencies were observed by Okumura et al. [9] in the IR spectra of the ion clusters of H_{2n+1}^+ ($n = 2$–7). They found that the frequency shift of H_{15}^+ relative to the monomer frequency is not too significant, which means that the apparent stability of H_{15}^+ could not be explained. In 1989, Bae et al. [10] observed shell structure for H_{2n+1}^+ ($n = 2$–8) sequentially grown on seed positive ions generated by electron impact ionization in a pulsed supersonic jet. They suggested a pentagonal bipyramid geometry with H_5^+ core ion for the extra stability of H_{15}^+.

Extensive theoretical studies for H_5^+ and larger clusters have been performed to determine their stabilities and structures [11–22]. Molecular structures and the binding energies of H_{11}^+ and H_{13}^+ were predicted at the self-consistent field (SCF) level of theory by Huber [15] in 1980, and at the CISD level of theory including electron correlation effect by Farizon et al. [17] in 1992. Nagashima and Morokuma [18] performed a study of H_{2n+1}^+ ($n = 4$–17) using classical Monte Carlo method in the same year. They found magic numbers in the stabilization energy at $n = 3, 6, 9, 12,$ and 15, which are consistent with the H_3^+ core structures completed with one to five layers of $(H_2)_3$ coordination shells. In 1997, theoretical investigations for the structures and binding energies of hydrogen clusters, up to H_{13}^+, were per-

formed at the HF, CISD, and DFT levels of theory by Chermette et al. [19].

The first ab initio calculation for H_{15}^+ and larger hydrogen clusters was performed by Diekmann et al. [20] at the TZP CISD level of theory in 1996. More recently, the molecular structures and binding energies of H_{2n+1}^+ (up to $n = 10$) were computed using the modified G2 method by Ignacio and Yamabe [21] in 1998. They concluded that the magic number $n = 7$ in the of H_{2n+1}^+ cluster is not effective based on their calculation. This result is not consistent with previous theoretical predictions and experimental observation. In 1999, the structures and energetics of three conformers of H_{15}^+ with C_s, D_{3h}, and C_{3v} symmetries were predicted using a DFT especially designed for hydrogen clusters [B3(H)] by Farizon et al. These investigators predicted that the C_s and C_{3v} structures are true minima, while the D_{3h} structure is a transition state [22]. Also, the C_s structure is a little more stable than the C_{3v} structure; however, the energy difference is only 0.7 kcal · mol (0.03 eV). This dissociation energy is kept similar for H_{11}^+ and H_{13}^+ groups, which implies that H_{15}^+ does not show an enhanced stability, which is consistent with Edgar's conclusion. There is still a question as to why H_{15}^+ has been found to be the most abundant ion cluster in the experiment. To our knowledge, the vibrational frequencies of H_{17}^+ cluster have not yet been reported either theoretically or experimentally.

In this work, the geometrical parameters and dissociation energies for H_{2n+1}^+ ($n = 5$–8) clusters have been investigated using high-level ab initio quantum mechanical techniques with various basis sets and SCF, CCSD, and CCSD(T) methods. Harmonic vibrational frequencies are also predicted at the SCF and CCSD levels of theory with various basis sets to confirm that the optimized geometries are true minima or transition states. The dissociation energies, D_e, for H_{2n+1}^+ ($n = 5$–8) have been predicted using energy difference at each optimized geometry. Zero-point vibrational energies (ZPVEs) have been considered to compare with experimental dissociation energies, D_0.

Theoretical Approach

The basis sets used in this study are of DZ plus polarization (DZP), and triple zeta plus polarization (TZ2P) quality. The DZ basis set consists of the standard Huzinaga [23] and Dunning [24] ($4s/2s$) set for hydrogen. The DZP basis is DZ plus a single
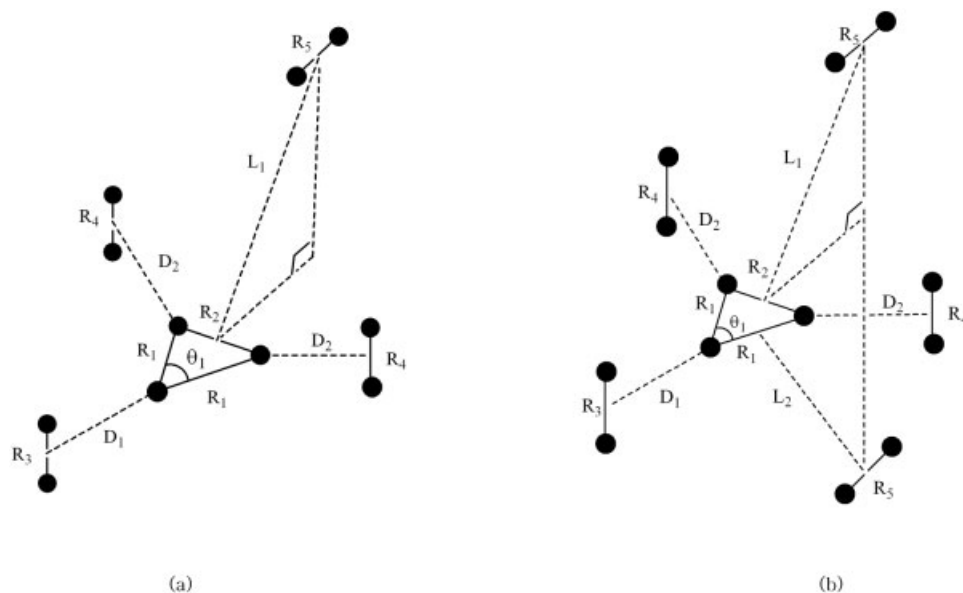
FIGURE 1. Predicted geometrical structures of (a) H_{11}^+ in C_s symmetry and (b) H_{13}^+ in C_s symmetry at the TZ2P CCSD(T) level of theory.

set of polarization p function on hydrogen with orbital exponent of $\alpha_p(H) = 0.75$. The TZ2P basis is of triple zeta (TZ) quality with two sets of polarization p functions with orbital exponents $\alpha_p(H) = 1.5$, 0.375, while the TZ basis consists of the Huzinaga [23] and Dunning [25] $(5s/3s)$ set for H. In addition, aug-cc-pVTZ and aug-cc-pVQZ basis sets were employed to test the basis set effects of d- and f-type functions on the geometry optimization for hydrogen clusters [26, 27]. The numbers of basis functions are 85 and 153 with the DZP and TZ2P basis sets for H_{17}^+, and are 253 and 506 with aug-cc-pVTZ and aug-cc-pVQZ for H_{11}^+, respectively.

The geometries of the H_{2n+1}^+ (n = 5–8) clusters were fully optimized at the SCF level of theory using an analytic technique [28] with DZP, and TZ2P basis sets. The aug-cc-pVTZ and aug-cc-pVQZ basis sets were only used for geometry optimization of H_{11}^+ at the SCF level of theory. The SCF equilibrium geometries were subsequently used as starting points to optimize structures at the CCSD level, which is the single and double excitation coupled cluster method, and at the CCSD(T) level of theory, which consists of CCSD with the effects of connected triple excitations included perturbatively [29]. Harmonic vibrational frequencies and ZPVEs for the equilibrium geometries of H_{2n+1}^+ (n = 5–8) clusters were evaluated using analytic second energy derivatives [30] at the SCF level and using finite displacements of analytic first gradients at the

CCSD level of theory. Computations with aug-cc-pVTZ and aug-cc-pVQZ basis sets and CCSD frequencies were carried out with the Gaussian 03 program package [31]; all other computations described above are carried out with the PSI-2 [32] suite of computer programs developed in Professor Schaefer's laboratory.

Results and Discussion

STRUCTURES

H_{11}^+ and H_{13}^+ Clusters

The geometrical indexes of the H_{11}^+ and H_{13}^+ clusters are shown in Figure 1, and their geometrical parameters at various levels of theory are shown in Table I. Theoretical calculations of H_{11}^+ revealed that three corners of the H_3^+ triangle are occupied by three H_2 molecules and added another H_2 molecule above the plane of the triangle. Optimized geometry shows C_s symmetry. The effects of increasing the basis set from DZP to TZ2P elongate significantly for the distances (D_1 and D_2) from the hydrogen in the H_3^+ plane to the center of H_2 subunit in the first solvation shell and decrease for the distance (L_1) between the deformed H_9^+ core and added H_2 subunit in the second solvation shell at correlated levels of theory such as CCSD and

TABLE I

Optimized geometrical parameters of H_{11}^+ and H_{13}^+ at various levels of theory.

| | H_{11}^+ | | | | | | | | | H_{13}^+ | | | | | |
| | SCF | | | | CCSD | | CCSD(T) | | | SCF | | CCSD | | CCSD(T) | |
sym (C_s)	DZP	TZ2P	aug-cc-pVTZ	aug-cc-pVQZ	DZP	TZ2P	DZP	TZ2P	sym (C_s)	DZP	TZ2P	DZP	TZ2P	DZP	TZ2P
R_1 (Å)	0.875	0.871	0.871	0.872	0.889	0.883	0.890	0.884	R_1(Å)	0.873	0.870	0.887	0.880	0.888	0.881
R_2 (Å)	0.877	0.873	0.873	0.874	0.893	0.886	0.895	0.888	R_2(Å)	0.878	0.873	0.895	0.887	0.896	0.889
R_3 (Å)	0.744	0.742	0.742	0.742	0.753	0.751	0.753	0.751	R_3(Å)	0.743	0.742	0.752	0.751	0.753	0.751
R_4 (Å)	0.743	0.741	0.742	0.742	0.753	0.751	0.753	0.752	R_4(Å)	0.743	0.742	0.753	0.751	0.753	0.752
R_5 (Å)	0.738	0.737	0.737	0.737	0.746	0.745	0.746	0.745	R_5(Å)	0.737	0.736	0.746	0.745	0.746	0.745
D_1 (Å)	1.784	1.809	1.821	1.821	1.679	1.707	1.672	1.698	D_1(Å)	1.832	1.852	1.693	1.714	1.685	1.705
D_2 (Å)	1.781	1.810	1.818	1.817	1.662	1.694	1.653	1.684	D_2(Å)	1.816	1.853	1.653	1.696	1.643	1.684
L_1 (Å)	2.726	2.655	2.671	2.671	2.633	2.491	2.624	2.474	L_1(Å)	3.075	2.972	2.992	2.880	2.980	2.865
									L_2(Å)	2.817	2.747	2.656	2.551	2.647	2.536
θ (degree)	60.2	60.1	59.9	59.9	60.3	60.3	60.4	60.3	θ (degree)	60.4	60.3	60.6	60.5	60.7	60.5

CCSD(T). However, the basis set effects of d- and f-functions are not too significant as confirmed from the results with aug-cc-pVTZ and aug-cc-pVQZ basis set at the SCF level of theory. The H—H bond lengths (R_1 and R_2) in the H_3^+ core are predicted to be 0.884 and 0.888 Å, and the distances, D_1 and D_2 are predicted to be 1.698 and 1.684 Å at the TZ2P CCSD(T) level of theory. The distance (L_1) from the deformed H_9^+ core to added H_2 subunit in the second solvation shell is predicted to be 2.474 Å. The H—H bond length (R_5) of H_2 subunit in the second solvation shell is predicted to be 0.745 Å, which is very close to the 0.741 Å of free H_2, while the bond distances (R_3 and R_4) of H_2 in the first solvation shell is 0.751 and 0.752 Å. This implies that the H_2 subunit in the second solvation shell is very weakly bound to the H_9^+ core.

H_{13}^+ is composed by attaching of one more H_2 molecule to the H_{11}^+. Two H_2 subunits in the second solvation shell of H_{13}^+ are weakly bound above and below the H_9^+ plane, parallel to the plane but off center. The H—H bond lengths (R_1 and R_2) in the H_3^+ ring are predicted to be 0.881 and 0.889 Å and the distances (D_1 and D_2) from the hydrogen in the H_3^+ plane to the center of H_2 subunit in the first solvation shell are calculated to be 1.705 and 1.684 Å. One (L_1, 2.865 Å) of the distances from the H_9^+ core to the two H_2 subunits in the second solvation shell is predicted to be significantly longer than that of H_{11}^+ and the other, L_2 (2.536 Å) is 0.062 Å longer. The H—H distance (R_5) of the farthest H_2 from the H_9^+ plane in H_{13}^+ is predicted to be 0.745 Å, which is the same as that in H_{11}^+. Ignacio and Yamabe [21] predicted the H—H distances in H_3^+ as 0.885 and 0.894 Å and the H_3^+—H_2 distances (D_1 and D_2) as 1.722 and 1.683 Å at the MP2/6-311** level in 1998.

H_{15}^+ (C_{3v}, C_s, and C_1 Symmetry) Clusters

In 1999, three conformers of H_{15}^+ with C_s, D_{3h}, and C_{3v} symmetries were predicted by Farizon et al. [22]. They predicted that the C_s and C_{3v} structures are true minima, while the D_{3h} structure is a transition state. In this study, we found another true minimum, C_1 structure, which has the lowest energy among three conformers of H_{15}^+. The C_{3v} structure of H_{15}^+ can be thought of as the addition of three H_2 molecules to a H_9^+ core on the same side as shown in Figure 2(a). The optimized geometrical parameters at various levels of theory are shown in Table II. The H—H bond length (R_1) in H_3^+ core is predicted to be 0.881 Å at the TZ2P CCSD(T) level of theory. And H—H bond distances for R_2 and R_3 are predicted to be 0.751 and 0.745 Å, which are not too different from those in H_{11}^+ and H_{13}^+ clusters. However, the distance (D_1) from the H_3^+ core to first solvation shell is calculated to be significantly longer (1.727 Å), while the distance (L_1) from the H_3^+ core to second solvation shell is decreased a little (2.400 Å). According to a recent report, in 1999, Farizon et al. [22] predicted R_1 of 0.886 Å, the distance H_3^+–H_2 (D_1) of 1.658 Å, and L_1 of 2.835 Å at the B3(H)/DFT level of theory.

Figure 3(b) shows the C_s structure built by the addition of two H_2 molecules on one side of the H_9^+ core and the last H_2 on the opposite side. These outer H_2 subunits in the second solvation shell are found to be off-centered with respect to the center of the H_3^+ core. The optimized geometrical parameters of H_{15}^+ with C_s symmetry also are compiled in Table II. The distances of R_1 and R_2 in the H_3^+ are predicted to be the same as 0.882 Å and the H—H bond lengths for R_3 (0.750 Å) and R_4 (0.751 Å) are
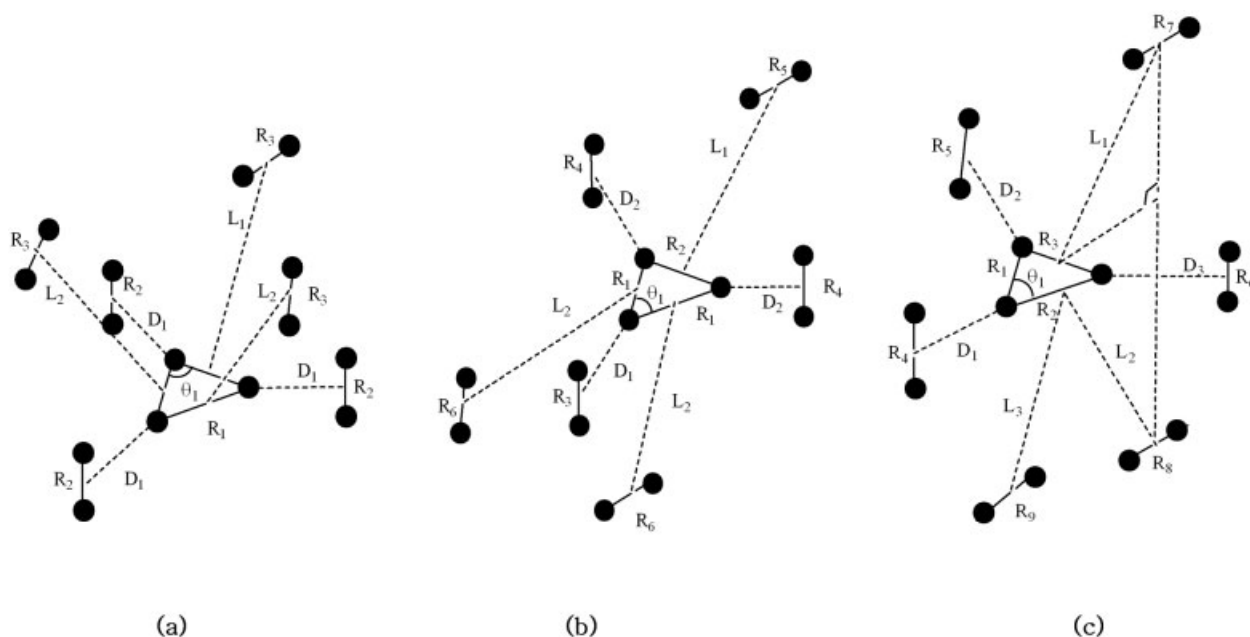
FIGURE 2. Optimized structures in (a) C_{3v}, (b) C_s, and (c) C_1 symmetries of H_{15}^+ at the TZ2P CCSD(T) level of theory.

found to be similar to those in H_{11}^+ and H_{13}^+ clusters. The H_2 molecules become farther from the H_3^+ core, the H—H bond lengths (R_5: 0.744 Å, R_6: 0.745 Å) decrease to be free H_2 molecules. The distances D_1 and D_2 are calculated to be 1.727 and 1.696 Å, which

are increasing from H_{11}^+ going to H_{15}^+. However, the distances L_1 and L_2 of 2.584 and 2.482 Å, respectively, are slightly decreased from H_{13}^+ going to H_{15}^+. The structure in C_s symmetry of H_{15}^+ is predicted as a local minimum and the most stable structure by

TABLE II

Optimized geometrical parameters at various levels of theory: H_{15}^+ (C_{3v}); H_{15}^+ (C_s); H_{15}^+ (C_1).

			R_1 (Å)	R_2 (Å)	R_3 (Å)	R_4 (Å)	R_5 (Å)	R_6 (Å)	R_7 (Å)	R_8 (Å)	R_9 (Å)	D_1 (Å)	D_2 (Å)	D_3 (Å)	L_1 (Å)	L_2 (Å)	L_3 (Å)	θ (degree)
	SCF	DZP	0.874	0.743	0.747							1.809			2.831	2.715		60.0
		TZ2P	0.869	0.741	0.737							1.863			2.597	2.623		60.0
H_{15}^+	CCSD	DZP	0.888	0.752	0.746							1.684			2.624	2.624		60.0
(C_{3v})		TZ2P	0.880	0.750	0.745							1.739			2.417	2.417		60.0
	CCSD(T)	DZP	0.889	0.752	0.746							1.674			2.613	2.616		60.0
		TZ2P	0.881	0.751	0.745							1.727			2.400	2.400		60.0
	SCF	DZP	0.873	0.873	0.738	0.743	0.737	0.743				1.817	1.781		2.844	2.791		60.2
		TZ2P	0.870	0.870	0.740	0.741	0.736	0.736				1.855	1.826		2.828	2.700		60.0
H_{15}^+	CCSD	DZP	0.888	0.888	0.752	0.753	0.746	0.746				1.698	1.661		2.711	2.692		60.3
(C_s)		TZ2P	0.880	0.880	0.750	0.750	0.744	0.745				1.739	1.704		2.604	2.501		60.0
	CCSD(T)	DZP	0.889	0.889	0.752	0.753	0.746	0.746				1.689	1.651		2.700	2.684		60.3
		TZ2P	0.882	0.882	0.750	0.751	0.744	0.745				1.727	1.696		2.584	2.482		60.0
	SCF	DZP	0.871	0.874	0.876	0.743	0.743	0.743	0.738	0.738	0.737	1.792	1.803	1.790	2.821	2.778	2.746	60.2
		TZ2P	0.868	0.870	0.867	0.742	0.740	0.741	0.736	0.737	0.736	1.895	1.801	1.875	2.653	2.513	2.706	59.8
H_{15}^+	CCSD	DZP	0.885	0.888	0.892	0.752	0.753	0.753	0.746	0.746	0.746	1.668	1.689	1.672	2.710	2.694	2.646	60.4
(C_1)		TZ2P	0.877	0.882	0.879	0.751	0.750	0.750	0.745	0.745	0.745	1.774	1.691	1.738	2.457	2.374	2.513	59.9
	CCSD(T)	DZP	0.893	0.889	0.888	0.753	0.753	0.752	0.746	0.746	0.746	1.657	1.647	1.687	2.856	2.717	2.715	59.8
		TZ2P	0.878	0.883	0.880	0.752	0.750	0.751	0.745	0.746	0.745	1.762	1.680	1.724	2.439	2.360	2.459	60.0
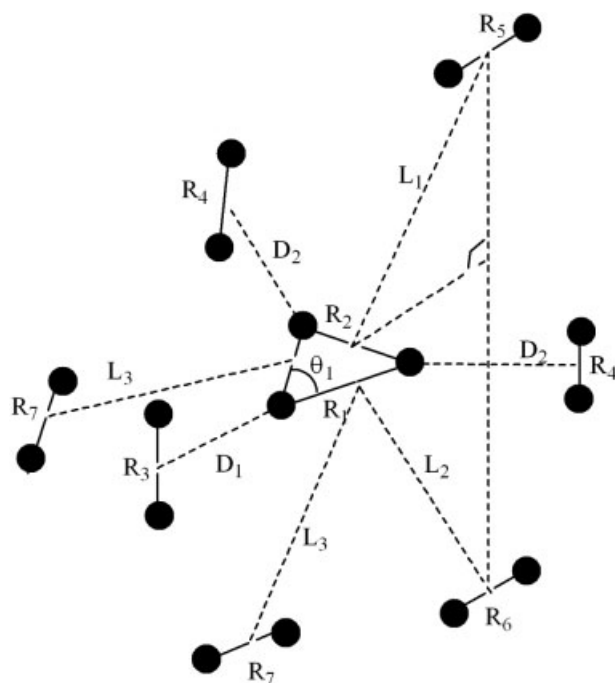
FIGURE 3. Optimized structure in C_1 symmetry of H_{17}^+ at the TZ2P CCSD(T).

Farizon et al. [22] in 1999. However, in this study, we conclude that C_s structure for H_{15}^+ is slightly more stable than C_{3v}, but is a transition state at the TZ2P CCSD level of theory.

As shown in Figure 2(c), the structure of H_{15}^+ with C_1 symmetry is formed by addition of one H_2 molecule, which lies below the H_9^+ unit and perpendicular to the H_3^+ plane, to the H_{13}^+. The geometrical parameters in C_1 symmetry of H_{15}^+ are predicted to be 0.878, 0.883, and 0.880 for R_1–R_3, 0.752, 0.750, and 0.751 for R_4–R_6, and 0.745, 0.746, and 0.745 Å for R_7–R_9, respectively. The distances (D_1, D_2, and D_3) from the H_3^+ core to the first solvation shell are predicted to be 1.762, 1.680, and 1.724 Å, respectively. The distances (L_1, L_2, and L_3) from the H_3^+ core to the second solvation shell are predicted to be 2.439, 2.360, and 2.459 Å, respectively. The interesting result is that the C_s structure has been regarded as a global minimum by Farizon et al. [22] in 1999. However, we conclude that the C_1 structure of H_{15}^+ is the global minimum from our result at the TZ2P CCSD(T) level of theory.

H_{17}^+ Cluster

As shown in Figure 3, the structure of H_{17}^+ is built by addition of one H_2, which lies below the H_9^+

unit, to the H_{15}^+ with C_s symmetry. The geometrical parameters of H_{17}^+ are predicted to be 0.880 and 0.884 for R_1–R_2, 0.750 and 0.751 for R_3–R_4, and 0.751, 0.745, and 0.745 Å for R_5–R_7, respectively as listed in Table III. Distances D_1 and D_2 are calculated to be 1.737 and 1.709 Å, which are the distances from the H_3^+ core to the first solvation shell. Distances (L_1, L_2, and L_3) from the H_3^+ core to the second solvation shell are predicted to be 2.629, 2.475, and 2.471 Å, respectively, at the TZ2P CCSD(T) level of theory. Ignacio and Yamabe [21] predicted the H—H distances in H_3^+ as 0.885 and 0.890 Å and the H_3^+–H_2 distances (D_1 and D_2) as 1.724 and 1.695 Å at the MP2/6-311** level in 1998.

VIBRATIONAL FREQUENCIES

Vibrational frequencies were predicted by the SCF and CCSD methods with DZP and TZ2P basis sets. The harmonic vibrational frequencies (cm^{-1}) and IR intensities (in km/mol) of H_{11}^+, H_{13}^+, $H_{15}^+(C_s)$, $H_{15}^+(C_1)$, $H_{15}^+(C_{3v})$, and H_{17}^+ at the TZ2P CCSD level of theory are listed in Table IV. As a result of the calculating vibrational frequencies, we confirm that H_{11}^+ is a true minimum. The harmonic vibrational frequency for outmost H_2 stretching, ω_1 is predicted to be 4372 cm^{-1}, which is relatively more like that (4410 cm^{-1}) of free H_2 molecule at the same level of theory, TZ2P CCSD. Three H_2 stretching modes, ω_2–ω_4, which are weakly bound to H_3^+, are calculated to be 4283–4289 cm^{-1}, while the most intense peak is 4283 cm^{-1}. Hydrogen stretching frequencies

TABLE III
Optimized geometrical parameters of H_{17}^+ at various levels of theory.

sym (C_s)	SCF		CCSD		CCSD(T)	
	DZP	TZ2P	DZP	TZ2P	DZP	TZ2P
R_1 (Å)	0.872	0.869	0.886	0.878	0.887	0.880
R_2 (Å)	0.875	0.871	0.891	0.883	0.892	0.884
R_3 (Å)	0.743	0.741	0.752	0.750	0.752	0.750
R_4 (Å)	0.743	0.741	0.752	0.750	0.753	0.751
R_5 (Å)	0.737	0.736	0.746	0.744	0.746	0.751
R_6 (Å)	0.737	0.736	0.746	0.745	0.746	0.745
R_7 (Å)	0.737	0.736	0.746	0.745	0.746	0.745
D_1 (Å)	1.822	1.862	1.700	1.749	1.690	1.737
D_2 (Å)	1.798	1.843	1.672	1.721	1.662	1.709
L_1 (Å)	2.876	2.904	2.741	2.651	2.729	2.269
L_2 (Å)	2.768	2.694	2.673	2.494	2.664	2.475
L_3 (Å)	2.772	2.714	2.665	2.492	2.656	2.471
θ (degree)	60.2	60.2	60.4	60.3	60.4	60.3

TABLE IV _____

Vibrational frequencies (in cm^{-1}) and infrared intensities (in parentheses in km · mol) of H_{11}^+, H_{13}^+, H_{15}^+ (C_s), H_{15}^+ (C_1), H_{15}^+ (C_{3v}), and H_{17}^+ at the TZ2P CCSD level of theory.

	TZ2P CCSD					
	H_{11}^+	H_{13}^+	H_{15}^+ (C_s)	H_{15}^+ (C_1)	H_{15}^+ (C_{3v})	H_{17}^+
ω_1	4372 (11.3)	4374 (4.1)	4381 (7.7)	4376 (8.8)	4373 (15.7)	4382 (7.2)
ω_2	4289 (1.6)	4374 (19.4)	4375 (18.0)	4373 (14.3)	4372 (13.0)	4377 (16.3)
ω_3	4284 (89.3)	4296 (4.6)	4373 (10.6)	4366 (18.2)	4372 (13.0)	4376 (11.2)
ω_4	4283 (94.8)	4290 (90.1)	4307 (24.0)	4311 (15.6)	4307 (7.0)	4375 (12.0)
ω_5	3291 (3.5)	4288 (76.0)	4297 (61.1)	4303 (86.9)	4303 (75.4)	4311 (16.4)
ω_6	2550 (812.2)	3311 (8.7)	4296 (68.8)	4289 (60.7)	4303 (75.4)	4306 (53.9)
ω_7	2532 (781.6)	2581 (766.5)	3331 (7.5)	3356 (20.1)	3349 (20.7)	4304 (70.8)
ω_8	801 (0.8)	2531 (730.4)	2595 (641.9)	2625 (574.3)	2590 (613.3)	3346 (9.7)
ω_9	797 (0.7)	782 (2.4)	2553 (697.6)	2551 (628.1)	2590 (613.3)	2597 (642.9)
ω_{10}	736 (0.9)	761 (0.0)	757 (0.2)	759 (3.4)	734 (12.9)	2579 (586.5)
ω_{11}	703 (5.0)	729 (3.8)	740 (4.1)	724 (0.7)	734 (12.9)	732 (5.7)
ω_{12}	611 (0.1)	703 (2.8)	689 (9.9)	680 (17.6)	674 (1.6)	718 (7.1)
ω_{13}	608 (8.0)	600 (0.1)	688 (3.8)	699 (25.2)	634 (0.0)	680 (2.1)
ω_{14}	469 (421.6)	580 (0.0)	572 (34.8)	584 (14.8)	580 (40.2)	653 (0.0)
ω_{15}	447 (486.9)	478 (365.6)	567 (17.4)	555 (2.2)	580 (40.2)	563 (46.0)
ω_{16}	429 (4.2)	432 (492.9)	437 (328.7)	473 (303.8)	412 (7.4)	556 (54.6)
ω_{17}	371 (30.0)	424 (0.2)	424 (150.2)	420 (17.3)	399 (52.2)	407 (35.1)
ω_{18}	249 (97.6)	366 (0.4)	395 (48.9)	394 (17.8)	399 (52.2)	396 (198.2)
ω_{19}	183 (4.3)	364 (45.1)	374 (147.5)	374 (31.7)	393 (7.2)	393 (92.1)
ω_{20}	169 (0.4)	263 (131.0)	371 (49.3)	359 (31.7)	345 (323.2)	384 (0.7)
ω_{21}	139 (0.1)	202 (6.4)	310 (70.3)	323 (353.5)	345 (323.2)	355 (132.1)
ω_{22}	130 (5.7)	199 (0.0)	250 (137.5)	276 (132.8)	230 (90.6)	354 (185.6)
ω_{23}	129 (9.6)	184 (0.0)	217 (4.3)	237 (23.5)	211 (3.7)	294 (81.1)
ω_{24}	118 (6.5)	160 (3.2)	206 (3.4)	204 (8.1)	211 (3.7)	233 (152.8)
ω_{25}	99 (3.2)	154 (0.0)	188 (1.4)	198 (7.6)	188 (13.9)	218 (8.0)
ω_{26}	93 (0.5)	151 (0.5)	180 (6.3)	192 (0.7)	188 (13.9)	209 (3.7)
ω_{27}	45 (8.4)	149 (6.5)	179 (13.6)	180 (9.7)	187 (42.0)	207 (1.1)
ω_{28}		122 (20.8)	169 (4.8)	155 (1.2)	170 (0.0)	193 (13.8)
ω_{29}		114 (1.8)	167 (2.0)	152 (3.4)	168 (0.5)	192 (16.9)
ω_{30}		98 (0.0)	152 (2.6)	148 (0.6)	168 (0.5)	183 (0.3)
ω_{31}		80 (0.0)	139 (1.6)	130 (3.2)	154 (2.9)	182 (5.7)
ω_{32}		48 (6.1)	135 (19.0)	116 (0.2)	154 (2.9)	174 (0.8)
ω_{33}		14 (9.7)	129 (3.8)	115 (10.7)	143 (0.0)	172 (0.4)
ω_{34}			112 (5.9)	111 (34.7)	128 (22.5)	159 (5.6)
ω_{35}			109 (6.9)	102 (3.5)	115 (0.5)	153 (0.9)
ω_{36}			83 (0.8)	86 (1.2)	115 (0.5)	153 (0.3)
ω_{37}			66 (7.6)	77 (2.9)	71 (1.1)	138 (3.2)
ω_{38}			17 (0.0)	61 (11.8)	71 (1.1)	135 (0.2)
ω_{39}			34i (3.0)	39 (1.5)	27 (0.0)	128 (10.8)
ω_{40}						117 (4.2)
ω_{41}						96 (4.6)
ω_{42}						72 (0.0)
ω_{43}						53 (2.7)
ω_{44}						42 (0.2)
ω_{45}						38 (0.3)

in the H_3^+ ring, ω_5–ω_7, are predicted to be 3291, 2550, and 2532. Other vibrational frequencies are located at <900 cm^{-1}, which include H—H stretch-

ing, bending, and torsional modes. The harmonic vibrational frequencies of H_{13}^+ are calculated to be ~4374 cm^{-1} for two outmost H_2 stretching modes

and ~4290 cm^{-1} for three H_2 stretching modes attached to H_3^+. Also, hydrogen stretching frequencies in the H_3^+ ring are predicted to be 3311, 2581, and 2531 cm^{-1}, which are not too different from those of H_{11}^+.

For H_{15}^+, three conformers, C_s, C_{3v}, and D_{3h}, have been known from the previous theoretical prediction [22]. Among them, the C_s and C_{3v} structures are predicted to be true minima, while the D_{3h} structure is calculated to be a transition state. In this study, the C_s structure of H_{15}^+ is predicted to be transition state, while C_{3v} and new C_1 structures are found to be true minima at the TZ2P CCSD level of theory. For the C_s structure, the frequency for outmost H_2 stretching, ω_1 is predicted to be 4381 cm^{-1}, which is closer to the value of 4410 cm^{-1} for the free H_2 molecule at the same level of theory. The vibrational frequencies in the H_3^+ ring, ω_5–ω_7, are increased by ~10 cm^{-1} compared to those for H_{13}^+, which implies that the bond strengths in the H_3^+ ring are slightly increasing by adding more H_2 molecules. This trend is also found in C_{3v} and C_1 structures of H_{15}^+. After applying the scaling factor of 0.94 based on the experimental anharmonic frequency, 4161 and TZ2P CCSD harmonic frequency, 4410 for the free H_2 molecule, strongest IR peaks for the stretching modes of H_2 subunits in the first solvation shell can be estimated to be 4026–4044 cm^{-1} for H_{11}^+–H_{15}^+ and are slightly increasing for larger clusters. This result is in excellent agreement with experimental observation of 4028–4048 cm^{-1} by Okumura et al. [9]. Also the scaled frequencies of 4110–4113 cm^{-1} for outer H_2 molecules in H_{11}^+–H_{15}^+ can be well matched with the experimental observation of the weak shoulders near 4080–4100 cm^{-1} in clusters larger than H_9^+ [9].

The harmonic vibrational frequencies for H_{17}^+ show all real numbers, implying a true minimum. The vibrational frequencies for four outmost H_2 stretching modes, 4375–4382 cm^{-1}, are becoming closer to that of the free H_2 molecule. For three H_2 stretching modes attached to H_3^+, the strongest peak is predicted to be 4304 cm^{-1}, which is not too different from that (4303 cm^{-1}) of H_{15}^+ with C_1 symmetry. The H_2 stretching frequencies in the H_3^+ ring are predicted to be 3346, 2597, and 2579 cm^{-1}. It will be interesting to compare the strong middle peaks of 2550, 2581, 2625, and 2597 cm^{-1} for H_{11}^+, H_{13}^+, H_{15}^+ (C_1 symmetry) and H_{17}^+, respectively. It increases, going from H_{11}^+ to H_{15}^+, but is decreasing

again for H_{17}^+. This implies that the H_3^+ ring in H_{15}^+ is more tightly bound to each other.

DISSOCIATION ENERGIES AND ZERO-POINT VIBRATIONAL ENERGIES

Dissociation energies and ZPVEs of H_{11}^+–H_{17}^+ are listed in Table V. The dissociation energies, D_e, for H_{2n+1}^+ ($n = 5$–8) have been predicted using energy differences at each optimized geometry

$$D_e(H_{11}^+) = E(H_{11}^+) - \{E(H_9^+) + E(H_2)\}$$

and ZPVEs have been considered to compare with experimental dissociation energies, D_0. In this study, the harmonic vibrational energy was performed at the TZ2P CCSD level of theory and corrected the anharmonicity using a scaling factor of 0.94, as described above. It was symbolized as Δ(ZPVE)*. The basis set effect for the dissociation energies at both CCSD and CCSD(T) levels seems significant.

At the TZ2P CCSD(T) level of theory, the dissociation energies (D_e) are predicted to be 1.69 for H_{11}^+, 1.65 kcal/mol for H_{13}^+, 1.65 kcal · mol for H_{15}^+ (C_1 symmetry), and 1.46 kcal · mol for H_{17}^+. The calculated dissociation energies are in excellent agreement with the experimental values obtained by Hiraoka [8] except for H_{17}^+. His experiment was performed in a wide range of temperature (330–25 K), which means that the measured may be different with standard-state values of H_{2n+1}^+. The experimental values should be between our ZPVE corrected values and the values without ZPVE correction. Therefore we compare our predicted dissociation energies without ZPVE correction with experimental values. The ZPVE-corrected dissociation energies of 0.44, 0.48, 0.52, and 0.34 kcal · mol for H_{11}^+, H_{13}^+, H_{15}^+ (C_1 symmetry), and H_{17}^+, respectively. The increment of the dissociation energy for H_{15}^+ relative to the H_{13}^+ cluster is 0.04 kcal · mol, and this is too small to say that there is the extra stability of the H_{15}^+ cluster.

Conclusions

The geometrical parameters, vibrational frequencies, and dissociation energies for H_{2n+1}^+ ($n = 5$–8) clusters have been investigated using high-level ab initio quantum mechanical techniques with large basis sets. Harmonic vibrational frequencies are also determined at the SCF and CCSD levels of

TABLE V

Absolute energies (E, in hartree), dissociation energies (D_e, in kcal · mol) and zero-point vibrational energies (in kcal · mol) of H_{11}^+–H_{17}^+ at various levels of theory.

		H_2	H_9^+	H_{11}^+	H_{13}^+	H_{15}^+ (C_s)	H_{15}^+ (C_1)	H_{15}^+ (C_{3v})	H_{17}^+
DZP CCSD	E	−1.166708	−4.859422	−6.027975	−7.196432	−8.364803	−8.364817	−8.364723	−9.533153
	$D_e(D_0)$			1.15 (0.05)	1.10 (0.17)	1.04 (−0.09)	1.05 (−0.02)	0.99 (−0.08)	1.05 (0.11)
TZ2P CCSD	E	−1.170805	−4.877830	−6.051222	−7.224546	−8.397525	−8.397845	−8.397666	−9.570665
	$D_e(D_0)$			1.62 (0.37)	1.58 (0.41)	1.36 (0.39)	1.57 (0.44)	1.45 (0.27)	1.37 (0.25)
DZP CCSD(T)	E	−1.166708	−4.859999	−6.028587	−7.197079	−8.365499	−8.365486	−8.365412	−9.533888
	$D_e(D_0)$			1.18 (0.08)	1.12 (0.19)	1.07 (−0.06)	1.07 (0.00)	1.02 (−0.05)	1.07 (0.13)
TZ2P CCSD(T)	E	−1.170805	−4.878598	−6.052095	−7.225526	−8.398635	−8.398955	−8.398792	−9.571919
	$D_e(D_0)$			1.69 (0.44)	1.65 (0.48)	1.45 (0.48)	1.65 (0.52)	1.54 (0.36)	1.46 (0.34)
Previous theories				(1.47)[a]	(1.58)[a]		(1.27)[a]		(1.39)[a]
						0.75[b]		0.68[b]	
				0.87[c]	1.04[c]				
Experiments				1.72 ± 0.1[d]	1.64 ± 0.1[d]		1.54 ± 0.1[d]		0.88 ± 0.1[d]
DZP CCSD	ZPVE	6.41	39.76	47.34	54.74	62.34	62.29	62.29	69.70
	Δ(ZPVE)*			1.10	0.93	1.13	1.07	1.07	0.94
TZ2P CCSD	ZPVE	6.30	39.44	47.07	54.61	61.94	62.11	62.17	69.60
	Δ(ZPVE)*			1.25	1.17	0.97	1.13	1.18	1.12

[a] Ref. [21].
[b] Ref. [22].
[c] Ref. [19].
[d] Ref. [8].
Δ(ZPVE)*, obtained from ZPVE applied anharmonicity scaling factor of 0.94.

theory with various basis sets to confirm that the optimized geometries are true minima or transition states. The C_1 structure for H_{15}^+ was predicted to be a global minimum in this study. The C_s and C_{3v} structures for H_{15}^+ estimated to be local minima in the past theoretical investigation are predicted to be a transition state for C_s and a local minimum for C_{3v} structure at the TZ2P CCSD level of theory. The strongest IR peaks for the stretching modes of H_2 subunits in first solvation shell are estimated to be $4026-4044$ cm^{-1} for H_{11}^+–H_{15}^+ and are slightly increasing for larger clusters, in excellent agreement with experimental observation by Okumura et al. [9]. Also, the scaled frequencies of $4110-4113$ cm^{-1} for outer H_2 molecules in H_{11}^+–H_{15}^+ can be well matched with the experimental observation of the weak shoulders near $4080-4100$ cm^{-1} in clusters larger than H_9^+ [9]. The dissociation energies, D_e, are predicted to be 1.69, 1.65, 1.65, and 1.46 kcal/ mol for H_{11}^+, H_{13}^+, H_{15}^+ (C_1 symmetry), and H_{17}^+, respectively, without ZPVE corrections and 0.44, 0.48, 0.52, and 0.34 kcal · mol for H_{11}^+, H_{13}^+, H_{15}^+ and H_{17}^+, respectively, with ZPVE corrections. The calculated dissociation energies without ZPVE correction are in excellent agreement with the experimental values obtained by Hiraoka [8] except for H_{17}^+.

References

1. Thomson, J. J Philos Mag 1912, 24, 209.
2. Krasoskii, V. I. Sov Astron 1958, 2, 775.
3. Drossart, P. Nature 1989, 340, 539.
4. Miller, S.; Tennyson, J.; Lepp, S.; Dalgarno, A. Nature 1992, 335, 420.
5. Clampitt, R.; Towland, L. Nature (London) 1968, 223, 815.
6. Van Deursen, A.; Reuss, J. Int J Mass Spectrom Ion Phys 1973, 11, 483.
7. Hiraoka, K.; Kebarle, P. J Chem Phys 1975, 62, 2267.
8. Hiraoka, K. J Chem Phys 1987, 87, 4048.
9. Okumura, M.; Yeh, L. I.; Lee, Y. T. J Chem Phys 1988, 88, 79.
10. Bae, Y. K.; Cosby, P. C.; Lorents, D. C. Chem Phys Lett 1989, 159, 214.
11. Poshuta, R. D.; Haugen, J. A.; Zetik, D. F. J Chem Phys 1969, 51, 3343.
12. Easterfield, J.; Linnett, J. W. Chem Commun 1970, 1, 64.
13. Harrison, S. W.; Massa, L. J.; Solomon, P. Nature (London) Phys Sci 1973, 245, 31.
14. Yamabe, S.; Hirao, K.; Kitaura, K. Chem Phys Lett 1978, 56, 546.
15. Huber, H. Chem Phys Lett 1980, 70, 353.
16. Yamaguchi; Gaw, J. F.; Schaefer, H. F. J Chem Phys 1983, 78, 4074.
17. Farizon, M.; Chermette, H.; Farizon-Mazuy, B. J Chem Phys 1992, 96, 1325.

18. Nagashima, U.; Morokuma, K. J Phys Chem 1992, 96, 4294.

19. Chermette, H.; Razafinjanahary, J.; Carrion, L. J Chem Phys 1997, 107, 10643.

20. Diekmann, B.; Borrmann, P.; Hilf, E. R. Surf Rev Lett 1996, 3, 253.

21. Ignacio, E. W.; Yamabe, S. Chem Phys Lett 1998, 287, 563.

22. Farizon, B.; Farizon, M.; Razafinjanahary, H.; Chermette, H. Phys Rev B 1999, 60, 3821.

23. Huzinaga, S. J Chem Phys 1965, 42, 1293.

24. Dunning, T. H. J Chem Phys 1970, 53, 2923.

25. Dunning, T. H. J Chem Phys 1971, 55, 716.

26. Dunning, T. H. J Chem Phys 1989, 90, 1007.

27. Kendall, R. A.; Dunning, T. H., Jr.; Harrison, R. J. J Chem Phys 1992, 96, 6796.

28. Yamaguchi, Y.; Osamura, Y.; Goddard, J. D.; Schaefer, H. F. A New Dimension to Quantum Chemistry: Analytic Derivative Methods in Ab Initio Molecular Electronic Structure Theory; Oxford University Press: New York, 1994.

29. Scheiner, A. C.; Scuseria, G. E.; Rice, J. E.; Lee, T. J.; Schaefer, H. F. J Chem Phys 1987, 87, 5361.

30. Saxe, P.; Yamaguchi, Y.; Schaefer, H. F. J Chem Phys 1982, 77, 5647.

31. Frisch, M. J.; Trucks, G. W.; Schlegel, H. B.; Scuseria, G. E.; Robb, M. A.; Cheeseman, J. R.; Montgomery, J. A., Jr.; Vreven, T.; Kudin, K. N.; Burant, J. C.; Millam, J. M.; Iyengar, S. S.; Tomasi, J.; Barone, V.; Mennucci, B.; Cossi, M.; Scalmani, G.; Rega, N.; Petersson, G. A.; Nakatsuji, H.; Hada, M.; Ehara, M.; Toyota, K.; Fukuda, R.; Hasegawa, J.; Ishida, M.; Nakajima, T.; Honda, Y.; Kitao, O.; Nakai, H.; Klene, M.; Li, X.; Knox, J. E.; Hratchian, H. P.; Cross, J. B.; Adamo, C.; Jaramillo, J.; Gomperts, R.; Stratmann, R. E.; Yazyev, O.; Austin, A. J.; Cammi, R.; Pomelli, C.; Ochterski, J.; Ayala, P. Y.; Morokuma, K.; Voth, G. A.; Salvador, P.; Dannenberg, J. J.; Zakrzewski, V. G.; Dapprich, S.; Daniels, A. D.; Strain, M. C.; Farkas, O.; Malick, D. K.; Rabuck, A. D.; Raghavachari, K.; Foresman, J. B.; Ortiz, J. V.; Cui, Q.; Baboul, A. G.; Clifford, S.; Cioslowski, J.; Stefanov, B. B.; Liu, G.; Liashenko, A.; Piskorz, P.; Komaromi, I.; Martin, R. L.; Fox, D. J.; Keith, T.; Al-Laham, M. A.; Peng, C. Y.; Nanayakkara, A.; Challacombe, M.; Gill, P. M. W.; Johnson, B.; Chen, W.; Wong, M. W.; Gonzalez, C.; Pople, J. A. Gaussian 03; Revision A.1; Gaussian: Pittsburgh, PA, 2003.

32. Janssen, C. L.; Seidl, E. T.; Scuseria, G. E.; Hamilton, T. P.; Yamaguchi, Y.; Remington, R. B.; Xie, Y.; Vacek, G.; Sherrill, C. D.; Crawford, T. D.; Fermann, J. T.; Allen, W. D.; Brocks, B. R.; Fitzgerald, G. B.; Fox, D. J.; Gaw, J. F.; Handy, N. C.; Laidig, W. D.; Lee, T. J.; Pitzer, R. M.; Rice, J. E.; Saxe, P.; Scheiner, A. C.; Schaefer, H. F. PSI 2.0.8; PSITECH: Watkinsvilles, GA, 1994.